

APPARENT ACTIVATION ENERGY OF SUBCRITICAL CRACK GROWTH OF SiC/SiC COMPOSITES AT ELEVATED TEMPERATURES - Y. S. Chou (Associated Western Universities, NW), M. M. Stackpoole and R. Bordia (University of Washington, Seattle), C. H. Henager, Jr., C. F. Windisch, Jr., and R. H. Jones (Pacific Northwest Laboratory^a).

OBJECTIVE

The purpose of this study is to investigate the environmental effect of oxygen-containing gases on the subcritical crack growth of continuous fiber (Nicalon "SiC") reinforced ceramic matrix (SiC) composites at elevated temperatures. This is a continuing project and the primary goal for this time period is to obtain an apparent activation energy for SiC/SiC materials with two different interfaces: carbon and boron nitride coatings.

SUMMARY

In the past six months, we have conducted studies of subcritical crack growth on SiC/SiC composite materials in a corrosive (O₂) as well as an inert (Ar) atmosphere for temperatures ranging from 800 to 1100°C. Two materials, one with ~1 μm carbon (C) interface and the other with ~0.5 μm boron nitride (BN), were investigated. Apparent activation energies (E_{act}) were determined from both the crack velocity and thermogravimetric analysis. In pure Ar, it was found that the apparent activation energy gradually increased with time, consistent with the development of steady-state bridging zone. The asymptotic value for E_{act} from crack growth data was found to be ~205 kJ/mol and ~234 kJ/mol for BN- and C-interface materials, respectively, in good agreement with published data (~200 kJ/mol) for creep of Nicalon fibers. In the presence of oxygen, E_{act} decreased to ~40-50 kJ/mol for C-interface and ~50-68 kJ/mol for BN-interface. Microstructural characterization of the oxidized samples indicated that the growth rate of the reaction front for BN-interface materials is an order of magnitude lower than for C-interface ones. At higher temperatures, a glassy phase was observed to seal off the BN-interface, whereas the C-interface remained open during all tests.

PROGRESS AND STATUS

Introduction

The brittle nature of monolithic ceramic materials can be greatly improved by incorporating strong continuous fibers into ceramic matrices [1-6]. By carefully controlling the interface and interphases, catastrophic failure can be avoided through progressive interfacial debonding, fiber bridging, and fiber pullout. Fracture toughness values as high as ~30 MPa√m have been reported for continuous fiber reinforced ceramic composites (CFCC) [5]. This allows the fiber-reinforced ceramic materials to be considered as a strong candidate for structural applications at elevated temperatures where monolithic ceramics would not be appropriate.

Recent development of high strength Nicalon (Si-O-C) fibers and Nicalon fiber-reinforced chemical vapor infiltration (CVI) processed SiC matrix composites have offered a great opportunity for structural applications at high temperature as well as for fusion reactor applications [7-10], primarily due to their low activation from irradiation. If, however, CFCCs are to be used in systems where long-term stability is required, a resistance to time-dependent crack growth (e.g., subcritical crack growth (SCG)) would be required. For monolithic SiC ceramics, subcritical crack growth has been studied by Tressler et al. [11-15], Henshall et al. [16], Larsen et al. [17], and Evans and Lange [18]. The high-temperature crack

^aPacific Northwest Laboratory is operated for the U.S. Department of Energy by Battelle Memorial Institute under Contract DE-AC06-76RLO 1830.

growth mechanism was suggested to be the viscous separation of an amorphous grain-boundary phase [11, 18].

For the CFCC materials such as SiC/SiC composites, Henager and Jones [19-21] have identified a K-independent region for "crack" (damage) propagation at elevated temperatures and attributed this behavior to the development of steady-state bridging zone [19-21]. It needs to be realized that the SiC/SiC fiber composites exhibited multiple cracking damage as well as microcrack damage during the SCG tests rather than the propagation of a single long crack. It would be more appropriate to use the term "damage" in this context rather than crack. The objective of this six-month work is to continue the study of SCG behavior by determining the apparent activation energy for damage growth in argon as well as in oxygen at elevated temperatures. Composites with both 1 μm C- and 0.5 μm BN-interface were examined.

Experimental

Composites consisting of Nicalon fiber cloth ($0^\circ/90^\circ$) and CVI β -SiC with C- and BN-interfaces were tested. The composites consist of eight plies and are approximately 4 mm in thickness. Interfaces of ~ 1.0 μm C or ~ 0.5 μm BN were deposited before the CVI infiltration process. Single-edge-notched-bend bars (SENB) with dimensions of 4 mm x 5.5 mm x 50 mm were tested in a fully articulated SiC bend fixture.

The SCG studies were performed using constant loading tests for times up to 1×10^5 s, giving the velocity of the "damage" zone from the notch root through the specimen for long times. The tests were conducted at temperatures ranging from 800°C to 1100°C in Ar and Ar plus varying O₂ levels. The specimens were typically loaded at an applied stress intensity of 9 to 10 MPa $\sqrt{\text{m}}$ to begin the test. Activation energy (E_{act}) was determined from the log-log plot of damage velocity versus 1/T. The details of the determination of damage velocity are given in Ref. 19. A typical specimen deflection versus time during one of the SCG tests is shown in Figure 1. The damage velocity at a specific time was determined by differentiating a third-order polynomial equation fit to the deflection versus time data.

Thermogravimetric analysis (TGA) was also conducted on SiC/SiC materials to determine the kinetics of interfacial reaction. TGA tests were conducted using approximately 4 mm x 4 mm x 8 mm bars cut from bend bars with only one exposed surface (area ~ 0.3 to 0.4 cm²). Tests were performed at temperatures ranging from 800 to 1100 °C for times from 3 to 24 hours using a Netzsch Analyzer (STA409) with a multi-gas controller (MKS 147) and a O₂ meter (Thermox). Samples after TGA tests were polished and characterized the reaction front using optical microscopy. The growth rate of the reaction front was averaged from the reacted section length divided by the total oxidation time.

Results

Figure 2 shows the apparent activation energy versus time for damage growth in SiC/BN/SiC composites in pure argon environment ($p\text{O}_2 < 1 \times 10^{-10}$ ppm). It is interesting to note that the apparent activation energy is not a constant but increases with time. Initially, E_{act} was about 170 kJ/mol and reached approximately 205 kJ/mol in 30000 seconds. Similar behavior was also observed for C-interface composites where E_{act} was found to be ~ 234 kJ/mol.

In the presence of oxygen, E_{act} was greatly reduced whereas the damage velocity increased appreciably. Figures 3 and 4 show the plots of E_{act} versus time for C-interface materials in Ar plus 5000 ppm pO₂ and for BN-interface materials in Ar plus 20000 ppm pO₂ environments, respectively. The apparent activation energy in oxygen is also not a constant for either interface as in the pure argon environment. In addition, the apparent activation energy tends to decrease at longer times and this decrease in E_{act} was more pronounced for C-interface materials than BN-interface ones. For example, E_{act} almost reached zero at 8000 s before the sample failed whereas BN-interface materials only dropped from 50 kJ/mol to about 42 kJ/mol before the sample failed.

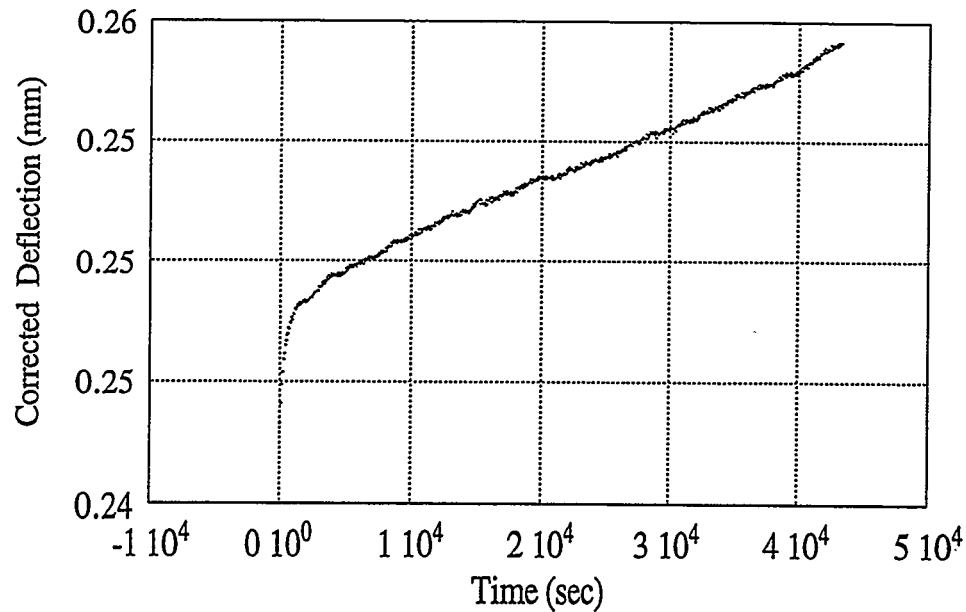


Fig. 1 Typical deflection versus time curve for SiC/SiC composites tested at elevated temperature with constant loading. Note that the damage velocity at a specific time was determined by differentiating the third-order polynomial equation fit to the data.

The apparent activation energy for reactions occurring in the presence of oxygen was also estimated from TGA data for both C- and BN-interface materials. Figures 5 and 6 show a typical plot of weight loss (normalized with respect to exposed area) as a function of time for BN-interface and C-interface materials in Ar with 20000 ppm pO_2 environment, respectively. It is evident that the weight loss is temperature dependent and increases with time. For BN-interface materials, the weight loss initially increases approximately linearly with time and then increases parabolically at longer times. A similar trend was observed for C-interface materials except that the weight loss is more rapid and no distinct parabolic region was observed. For both materials, as temperature increases, so does the weight loss except for the BN-interface materials at 1100°C where the weight loss is less than at 1000°C. By obtaining instantaneous slope (weight loss rate) from Figs. 5 and 6, the apparent activation energy was determined from plots of the slope versus $1/T$ at specific times. Figures 7 and 8 show the plot of apparent activation energy versus oxidation time for C- and BN-interface materials, respectively. For BN-interface materials, E_{act} was determined from 800 to 1000°C data compared to 800 to 1100°C for C-interface materials. The apparent activation energy versus time from TGA data for both materials exhibited a similar trend as that obtained from the damage growth data for SiC/BN/SiC composite (Figs. 3 and 4), i.e., there exists a maximum E_{act} and E_{act} decreases at longer times. It is worth noting that E_{act} decreases to a minimum value in shorter times at higher oxygen concentrations. Figure 9 shows the average reaction front growth rate as a function of pO_2 for C- and BN-interface materials. The growth rate for the C-interface is approximately an order of magnitude greater than BN-interface.

Discussion

It has been observed by Henager and Jones [19-21] that SiC/SiC composite materials either with a C- or BN-interface exhibited stage-II V-K curves at elevated temperatures in a pure argon environment, i.e., the damage velocity, is independent of applied stress intensity. In the presence of oxygen, the damage velocity increased with increasing oxygen partial pressure, and was attributed to the oxidation of the interface such that the load carrying ability was reduced. For CFCC materials, weak interfaces such as C

and BN will lead to debonding as cracks propagate around the fibers leaving behind fibers bridging the crack, which results in non-catastrophic failure. The development of steady-state bridging zones has been modeled successfully to demonstrate the development of stage-II V-K curves [20]. The current measurement of the apparent activation energy of damage velocity for SiC/BN/SiC materials in a pure Ar environment (Fig. 2) seems to be consistent with the development of steady-state bridging zone, such that the fibers behind the crack-tip control the SCG behavior. The asymptotic value for E_{act} in pure Ar is about 205 kJ/mol. Simon and Bunsell [9] have reported an activation energy for Nicalon fibers from tensile creep tests at 1280 to 1320 °C of 370 kJ/mol and 270 kJ/mol in Ar and in air, respectively. DiCarlo [22] recently reported a value of 500 ± 65 kJ/mol for Nicalon fiber creep activation energy using data from bend stress relaxation tests and presented a semi-empirical creep equation for larger creep strain region ($\epsilon > 1\%$) in which an effective activation energy of 200 kJ/mol was obtained. Our data (234 kJ/mol for C- and 205 kJ/mol for BN-interface materials) are in good agreement with the DiCarlo's data for larger creep strains. It needs to be realized that in addition to fiber creep there are other mechanisms present during the development of the bridging zone, such as fiber-matrix interface creep, time-dependent interface debonding, and roughness-induced stick-slip sliding during fiber pullout. All these processes are expected to play roles in affecting the SCG behavior and need to be further explored. Nevertheless, the current data of E_{act} seems to suggest that fiber creep is the dominant mechanism for SCG behavior in these materials.

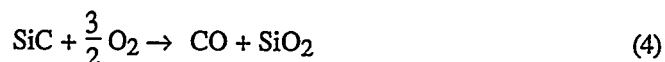
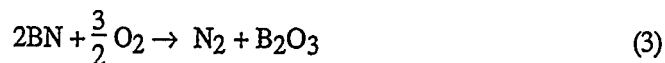
In the presence of oxygen, the damage velocities were found to be greater than in the pure Ar environment for both C- and BN-interface materials. In addition, region II in the V-K curves spans a smaller range of stress intensities. The apparent activation energy determined from the measured damage velocity was much smaller than in pure Ar, i.e., ≤ 50 kJ/mol. The oxidation of carbon in the presence of oxygen results in the formation of gaseous carbon oxides, with an overall weight loss, according to the following reactions



The activation energy for carbon oxidation varies from 30 to 123 kJ/mol and depends on the way it is formed. The carbon interface in this study was formed by cracking of CH_4 and has the typical laminar microstructure of pyrocarbon [23]. The E_{act} from this study is in reasonable agreement with the published data. It is worth noting that at longer times, E_{act} starts to drop abruptly (Fig. 3 for damage velocity data at $pO_2 = 5000$ ppm) suggesting that the C-interface was severely damaged (oxidized) such that little load was transferred to the bridging fibers. For very thin C-interfaces, e.g., 0.1 μm , it was found that the interface channels left after the carbon was oxidized were rapidly sealed off by silica at $T > 1000^\circ C$ [23]. In this study, however, the thickness of C-interface is $\sim 1.0 \mu m$ and Nicalon fibers, which are not stoichiometric SiC but Si-O-C, are known to release SiO and CO at elevated temperature and shrink. Therefore the interface channel could be kept open for continued oxygen attack. Similar behavior was also observed by Filipuzzi et al. [24] in 1-D SiC/C/SiC materials with a 1 μm thick C-interface. They found that carbon is totally consumed before silica can seal the interface channels. It is interesting to note that E_{act} obtained from the measured damage velocity is in good agreement with TGA tests (Fig. 7) although the stress states are different. The decrease of E_{act} at longer times for TGA tests is likely due to the passive oxidation of SiC matrix and fibers resulting in weight gain, which was attributed to the pore geometry change as well as the localized high concentration of CO_2 [23].

As for BN-interface materials, the measured E_{act} obtained was similar to that of the C-interface materials. The maximum E_{act} is about 50 kJ/mol from the damage velocity data and about 68 kJ/mol from the TGA results. The E_{act} from TGA tests was estimated from data taken from 800 to 1000°C. The

oxidation reaction corresponding to this activation energy remains to be identified. However, there are three possible oxidation reactions in SiC/BN/SiC materials



Equation 3 corresponds to oxidation of the BN interface and results in a glassy phase. Equation 4 corresponds to oxidation of the SiC matrix, and could produce glassy as well as crystalline forms of silica [25]. Equation 5 illustrates the active oxidation of SiC resulting in gaseous species and can only occur at low oxygen partial pressures. In addition, Nicalon fibers can also undergo thermal decomposition and gain or lose weight depending on whether oxidation occurs in a passive or active regime. Oxidation reactions (Eqs. 3 and 4) would result in weight gain whereas weight loss is observed for the active oxidation of SiC (Eq. 5). The current TGA results, i.e., weight loss in Fig. 5, suggest that either the SiC matrix undergoes active oxidation or the fibers decompose releasing SiO and CO. It is not clear why weight loss was observed since SiC would be in the passive regime and Nicalon fibers do not decompose below ~1250°C and even higher temperatures when embedded within a matrix. Nevertheless, at longer times and higher temperatures, silica has been observed to seal off the open pores for the BN-interface materials. The formation of a low viscosity glassy phase as well as the thermal decomposition of the interface will all reduce the load carrying capability of bridging fibers and led to lower E_{act} for SCG. In an inert environment, fiber decomposition only occurs around 1400°C and at higher temperature (1500°C) when embedded within SiC matrix [23].

CONCLUSIONS

An apparent activation energy was determined from growth of a damage zone during subcritical crack growth as well as from TGA data for C- and BN-interface materials. In a pure argon environment, the apparent activation energy from damage growth data is consistent with fiber creep results suggesting that the SCG behavior is determined by the creep of bridging fibers. In the presence of oxygen, E_{act} was substantially decreased to ~40-50 kJ/mol and ~50-70 kJ/mol for C- and BN-interface materials, respectively. For C-interface materials, E_{act} is consistent with the oxidation reaction of the interface suggesting the SCG behavior was dominated by the interfacial oxidation reaction. This is unclear for the BN-interface materials. Optically measured reaction front growth rates indicated that C-interface reacts much faster than BN-interface. In addition, a glassy phase was identified for BN-interface materials which sealed off the open pores after long time exposure at elevated temperatures in an oxygen-containing environment.

FUTURE WORK

1. To characterize the BN-interface materials after long time exposure in an oxygen-containing environment.
2. To fit our TGA and optically measured reaction front growth rate data with the existing 1-D model of Filipuzzi [25].

ACKNOWLEDGMENTS

The authors would like to acknowledge J. L. Humason for his testing expertise, and R. A. Adey and N. T. Saenz for microscopy. This work was supported by Basic Energy Sciences under the Department of Energy (DOE) Contract DE-AC06-76RLO 1830 with Battelle Memorial Institute that operates Pacific Northwest Laboratory for DOE.

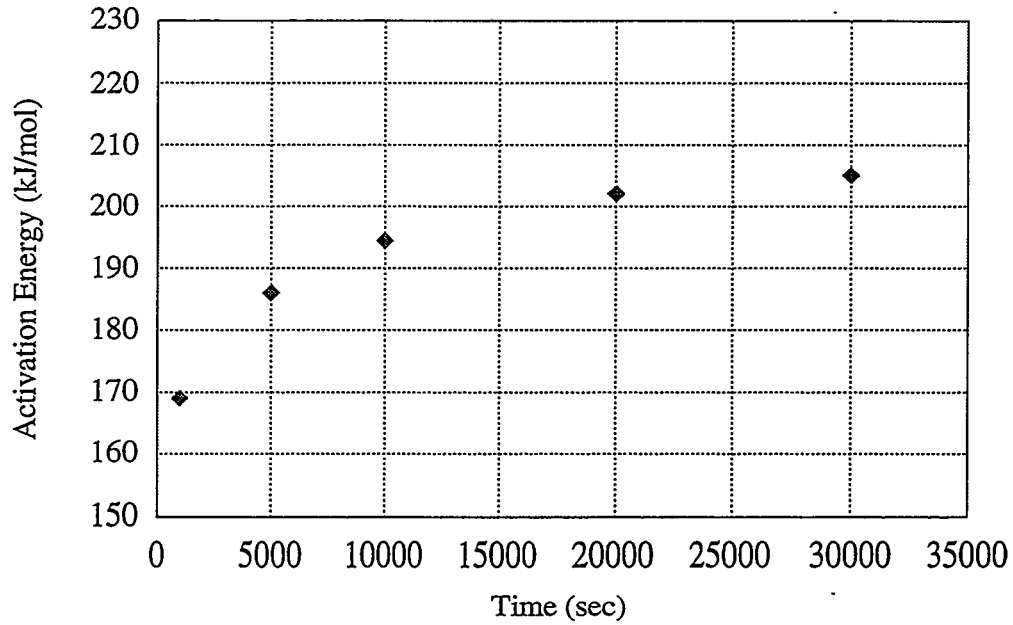


Fig. 2 Activation energy versus time plot for SiC/BN/SiC composites in pure Ar environment.

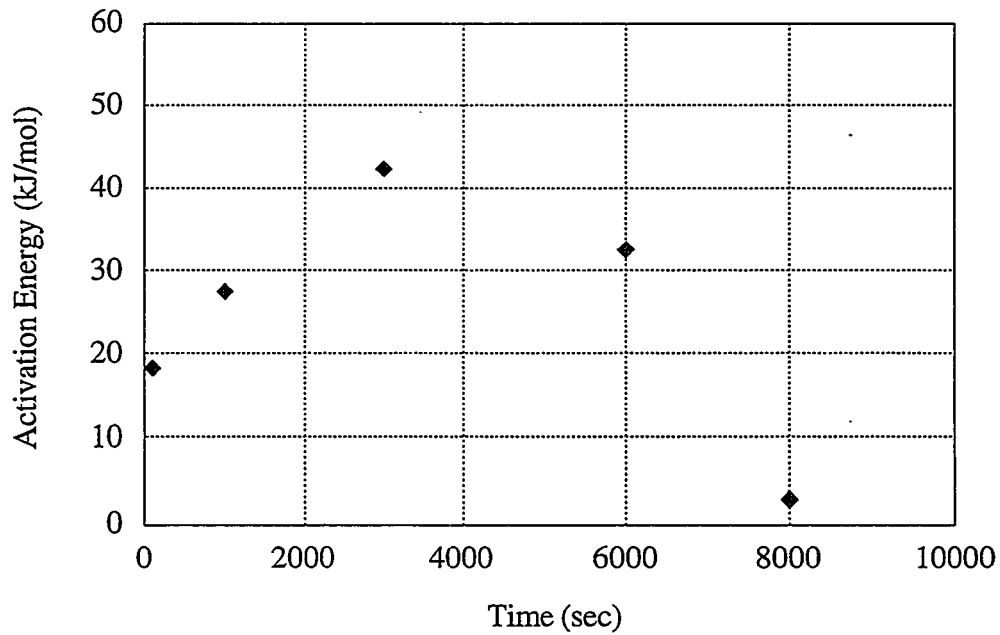


Fig. 3 Activation energy (determined from damage velocity) versus time plot for SiC/C/SiC composites in argon with 5000 ppm pO₂ environment.

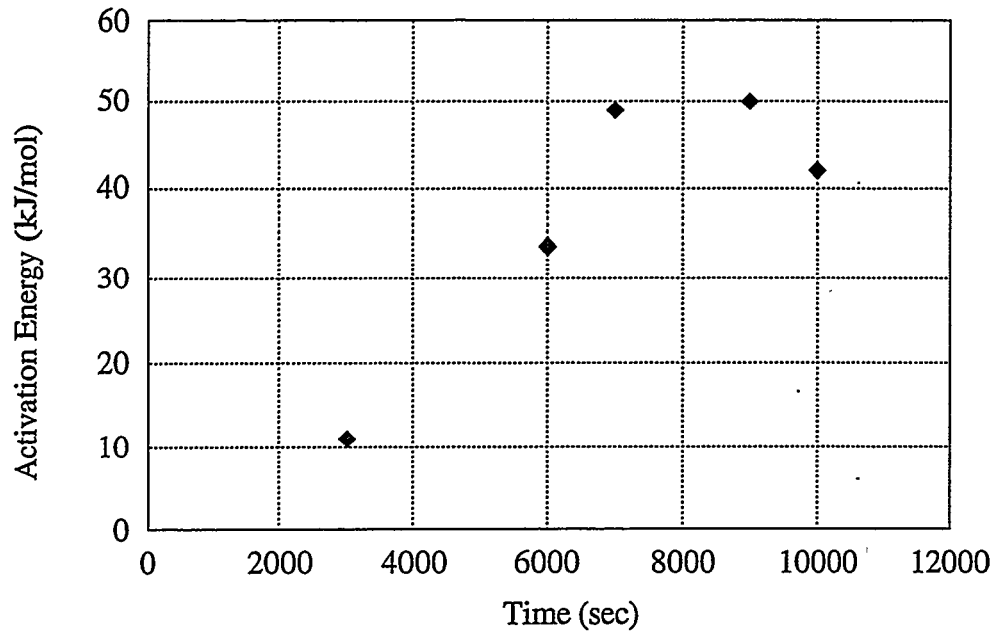


Fig. 4 Activation energy (determined from damage velocity) versus time plot for SiC/BN/SiC composites in argon with 20000 ppm pO_2 environment.

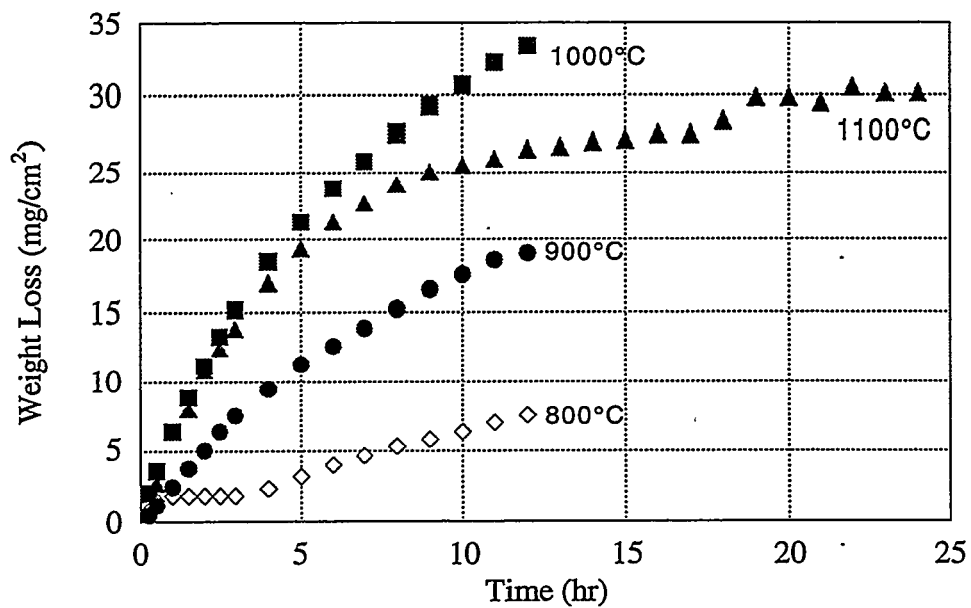


Fig. 5 Weight loss as a function of time for SiC/BN/SiC materials in Ar with 20000 ppm pO_2 environment.

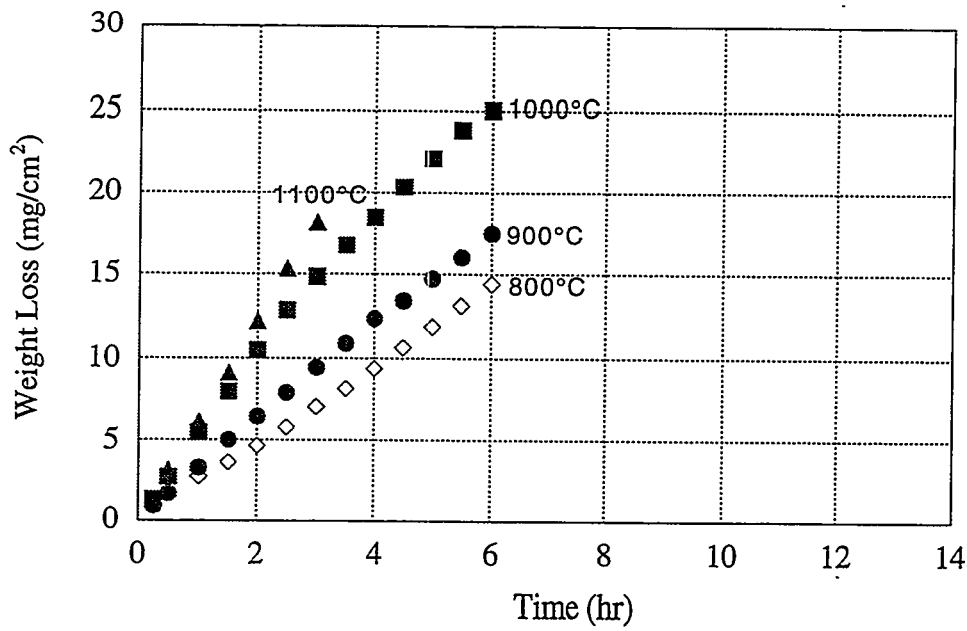


Fig. 6 Weight loss as a function of time for SiC/C/SiC materials in Ar with 20000 ppm pO_2 environment.

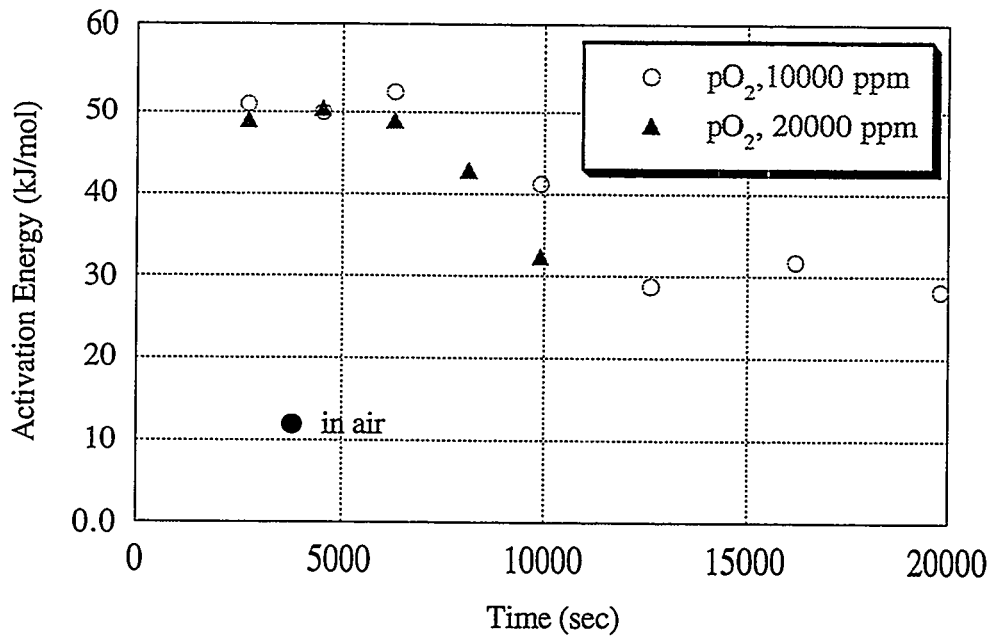


Fig. 7 Activation energy versus time plot obtained from TGA data (800-1100°C) for SiC/C/SiC composites in argon with 10000 ppm and 20000 ppm pO_2 environment.

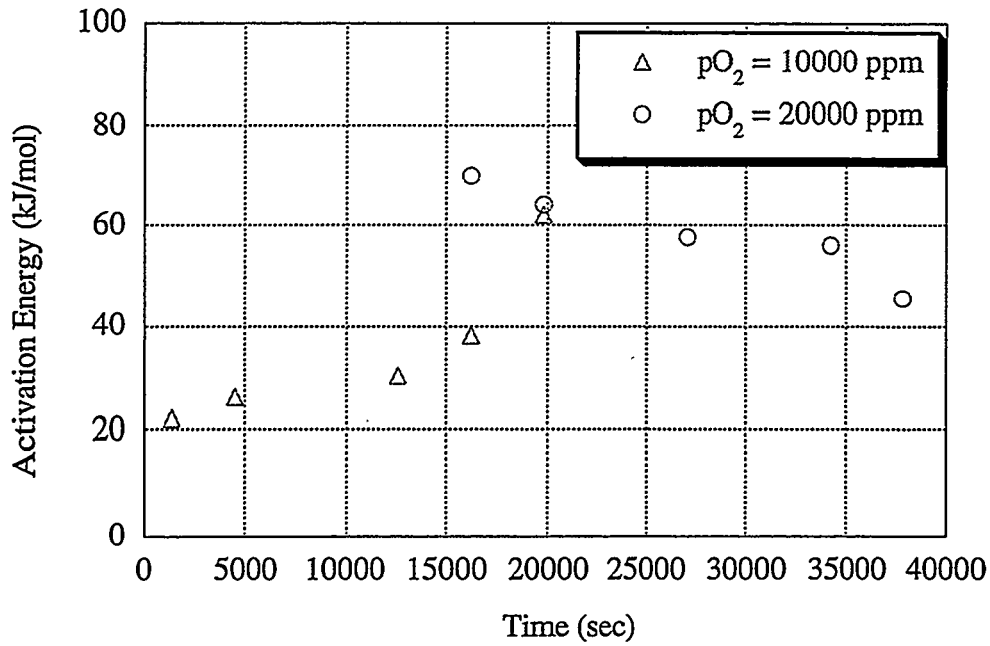


Fig. 8 Activation energy versus time plot obtained from TGA data (800-1000°C) for SiC/BN/SiC composites in argon with 10000 ppm and 20000 ppm pO_2 environment.

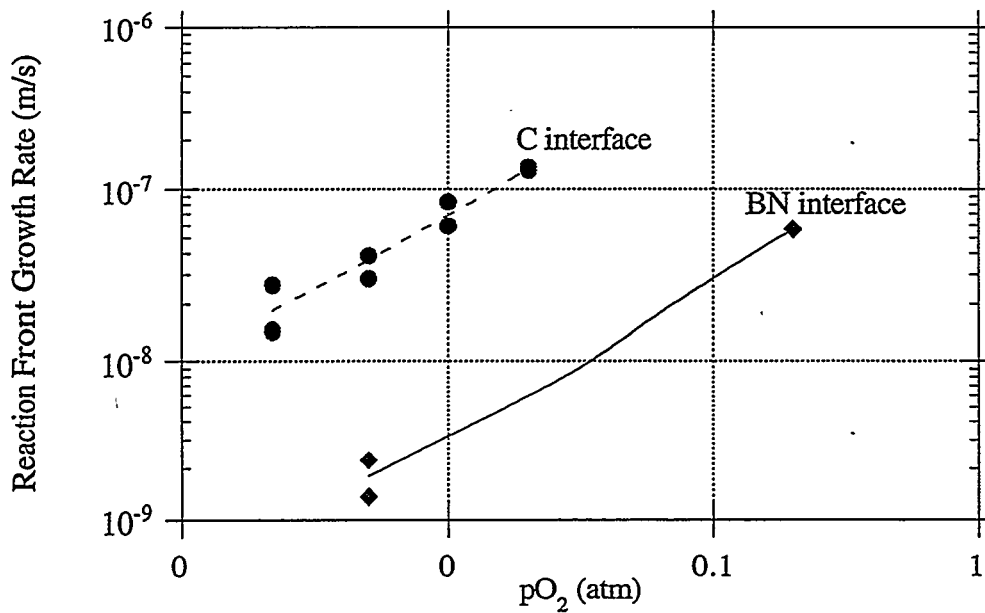


Fig. 9 Average reaction front growth rate (optically measured) versus pO_2 for C- and BN-interface materials.

REFERENCES

1. A. G. Evans and R. M. McMeeking, *Acta Metall.*, **34** [12] 2435-2441 (1986).
2. K. M. Prewo, *Am. Ceram. Soc. Bull.*, **68** [2] 395-400 (1989).
3. D. B. Marshall and A. G. Evans, *Acta Metall. Mater.*, **37** [10] 2567-2583 (1989).
4. H. C. Cao, E. Bischoff, O. Sbaizero, M. Rühle, A. G. Evans, D. B. Marshall, and J. J. Brennan, *J. Am. Ceram. Soc.*, **73** [6] 1691-1699 (1990).
5. K. M. Prewo and J. J. Brennan, *J. Mater. Sci.*, **17** 1201-6 (1982).
6. J. B. Davis, J. P. A. Löfvander, A. G. Evans, E. Bischoff, and M. L. Emiliani, *J. Am. Ceram. Soc.*, **76** [5] 1249-57 (1993).
7. T. Mah, N. L. Hecht, D. E. McCullum, J. R. Hoenigman, H. M. Kim, A. P. Katz, and H. A. Lipsitt, *J. Mater. Sci.*, **19** 1191-1201 (1984).
8. G. Simon and A. R. Bunsell, *J. Mater. Sci.*, **19** 3649-3657 (1984).
9. G. Simon and A. R. Bunsell, *J. Mater. Sci.*, **19** 3658-70 (1984).
10. R. H. Jones, C. H. Henager, Jr., and G. W. Hollenberg, *J. Nucl. Mater.*, **191-194** 75-83 (1992).
11. K. D. McHenry and R. E. Tressler, *J. Mater. Sci.*, **12** 1272-1278 (1977).
12. E. J. Minford and R. E. Tressler, *J. Am. Ceram. Soc.*, **66** [5] 338-340 (1983).
13. T. E. Easler, R. C. Bradt, and R. E. Tressler, *J. Am. Ceram. Soc.*, **64** [12] 731-734 (1981).
14. D. E. Carroll and R. E. Tressler, *J. Am. Ceram. Soc.*, **68** [3] 143-146 (1985).
15. K. D. McHenry, T. Yonushonis, and R. E. Tressler, *J. Am. Ceram. Soc.*, **59** [5-6] 262-263 (1976).
16. J. L. Henshall, D. J. Rowcliffe, and J. W. Edington, *J. Am. Ceram. Soc.*, **62** [1-2] 36-41 (1979).
17. D. C. Larsen, J. W. Adams, S. A. Bortz, and R. Ruh, *Fracture Mechanics of Ceramics*, vol. 6, Measurements, Transformations, and High-Temperature Fracture, edited by R. C. Bradt, A. G. Evans, D. P. H. Hasselman, and F. F. Lange, Plenum Press, New York, pp. 571-585 (1986).
18. A. G. Evans and F. F. Lange, *J. Mater. Sci.*, **10** 1659-1664 (1975).
19. C. H. Henager, Jr. and R. H. Jones, *Ceramic Eng. Sci. Proc.*, **13** [7-8] 411-419 (1992).
20. C. H. Henager, Jr. and R. H. Jones, *J. Am. Ceram. Soc.*, **77** [9] 2281-2394 (1994).
21. C. H. Henager, Jr. and R. H. Jones, *Ceramic Eng. Sci. Proc.*, **14** [7-8] 408-415 (1993).
22. J. A. DiCarlo, *Comp. Sci. Tech.*, **51** 213-222 (1994).
23. L. Filipuzzi, G. Camus, R. Naslain, and J. Thebault, *J. Am. Ceram. Soc.*, **77** [2] 459-66 (1994).
24. L. Filipuzzi and R. Naslain, *J. Am. Ceram. Soc.*, **77** [2] 467-80 (1994).
25. S. Baskaran and J. W. Halloran, *J. Am. Ceram. Soc.*, **77** [5] 1249-55 (1994).